

## A $\beta$ -Cyclodextrin/Siloxane Hybrid Polymer: Synthesis, Characterization and Inclusion Complexes

Camilla Abbehausen, André L. B. Formiga, Edvaldo Sabadini and Inez V. P. Yoshida\*

Institute of Chemistry, Campinas State University, CP 6154 13083-970 Campinas-SP, Brazil

Polímero híbrido derivado de siloxano e  $\beta$ -ciclodextrina ( $\beta$ -CD) foi obtido pela reação de  $\beta$ -CD com  $\gamma$ -isocianatopropiltrióxissilano (IPTS), seguido por reação de hidrólise/condensação, gerando uma resina de polissilsesquioxano modificada por  $\beta$ -CD (PSS- $\beta$ -CD). PSS- $\beta$ -CD foi caracterizado por espectroscopia infravermelha e ressonância magnética nuclear de  $^{13}\text{C}$  e  $^{29}\text{Si}$ . Este híbrido é amorfo e termicamente estável até 180 °C. PSS- $\beta$ -CD pode ser obtido também como filme e sua morfologia foi avaliada por microscopia eletrônica de varredura. A capacidade da  $\beta$ -CD ligada ao polímero em formar complexos de inclusão foi avaliada pela formação de um complexo de  $\beta$ -CD-fenolftaleína, utilizando espectroscopia UV-Vis. Mesmo sem mudanças no pH, a forma vermelha da fenolftaleína se converte na forma incolor quando PSS- $\beta$ -CD é imerso na solução. Cálculos teóricos (métodos AM1 e DFT) mostram que o complexo é formado pela inclusão do anel fenolato na cavidade da  $\beta$ -CD favorecendo a forma incolor da fenolftaleína por mais de 15 kcal mol $^{-1}$ .

A hybrid polymer derived from siloxane and  $\beta$ -cyclodextrin ( $\beta$ -CD) was obtained by reaction of  $\beta$ -CD with  $\gamma$ -isocyanatopropyltriethoxysilane (IPTS), followed by hydrolysis/condensation reactions, generating a  $\beta$ -CD-modified polysilsesquioxane resin (PSS- $\beta$ -CD). PSS- $\beta$ -CD hybrid was characterized by infrared spectroscopy and  $^{13}\text{C}$  and  $^{29}\text{Si}$  nuclear magnetic resonance. This hybrid was typically amorphous and thermally stable up to 180 °C. PSS- $\beta$ -CD was able to form films and its morphology was evaluated by scanning electron microscopy. The capability of  $\beta$ -CD grafted in the hybrid polymer to form inclusion complex was evaluated by the formation of a  $\beta$ -CD-phenolphthalein complex using UV-Vis spectroscopy. Even without changes in pH, the red form of phenolphthalein converts to the colorless one when PSS- $\beta$ -CD is immersed in the solution. Theoretical calculations (AM1 and DFT methods) show that the complex is formed through the inclusion of the phenolate ring into  $\beta$ -CD cavity, favoring the colorless form of phenolphthalein by more than 15 kcal mol $^{-1}$ .

**Keywords:** cyclodextrin, polysiloxanes, polysilsesquioxanes, inclusion complexes

### Introduction

Cyclodextrins (CD) correspond to natural and cyclic maltodextrins produced by the reaction of 4- $\alpha$ -glucanotransferase enzyme and an amide. Their structures are formed by  $\alpha$ -(1-4) hydroxyglucanopyranosidic units in a toroidal shape with an internal hydrophobic cavity that involves all the etherlike oxygens in  $\alpha$ -(1-4) glycosides bonds. The hydroxide groups of glucose units are arranged in two external rings up, which confer hydrophilic characteristics to the outer structure of the molecule. The most common cyclodextrins are  $\alpha$ -,  $\beta$ - and  $\gamma$ - with 6, 7 and 8 hydroxyglucanopyranosidic units, respectively.

CD have been used in a very large number of applications mainly due to their ability to form inclusion complexes with a variety of guest molecules, such as fatty acids and esters, aromatic compounds, aliphatic alcohols, antibiotics and proteins with aromatic amino acid residues.<sup>1</sup> These applications can be found in cosmetics,<sup>2</sup> food and flavours,<sup>3</sup> pharmaceuticals,<sup>4,5</sup> agriculture,<sup>6</sup> the chemical industries,<sup>7</sup> and environmental science,<sup>8</sup> among others.

CD, in their native state, are rigid molecules with limited utility in terms of availability of chemically useful functional groups. For this reason a number of researchers have looked for modifications, synthesizing CD derivatives, mainly by introduction of appropriate functional groups in the pristine structure. The modification is chosen according to the final application of the material and mostly of the

\*e-mail: valeria@iqm.unicamp.br

methodologies require reactions with the hydroxyl groups,<sup>9</sup> giving rise to CD-modified structures. CD-derivatives can be prepared as a single molecule or in the polymeric form.<sup>10</sup> CD-based polymers usually are prepared from the native CD with di- or poly-functional molecules, such as: hexamethylenediisocyanate, epichlorohydrin and poly(vinylalcohol).<sup>11</sup>

The introduction of CD in the structure of several polymers has been studied by combining the ability of CD to form inclusion complexes and the particular characteristics of each polymer, such as pharmacokinetics profile, film forming ability, transparency to UV-Vis light, porosity, and other properties that allow the development of high performance materials to be applied in different fields, such as stationary phases of chromatographic columns,<sup>12</sup> chemical sensors,<sup>13</sup> special filters,<sup>8</sup> drug delivery<sup>14</sup> and others.<sup>15</sup>

Inorganic polymers such polysiloxanes have a number of interesting properties such as high oxygen permeability, high temperature and chemical stabilities, low toxicity and biocompatibility.<sup>16</sup> These properties have inspired the design of new and unique materials by combining these polymers with special molecules.<sup>17,18</sup> In the past few years, numerous silica and/or siloxane based organic-inorganic polymers have been employed to produce hybrid materials with biomolecules, such as: proteins,<sup>19</sup> enzymes,<sup>20</sup> phospholipids<sup>21</sup> and also entire cells.<sup>22</sup> Typically, these materials are synthesized *via* the sol-gel technique, particularly from alkoxyxilanes (RSi(OR')<sub>3</sub>) precursors. This approach is compatible with biomolecules or labile molecules due to its mild conditions of temperature and pH, avoiding degradation or denaturation of the biomaterial. In addition, the resulting transparent glass like material allows the use of spectroscopic techniques to study the structure of the aggregate or encapsulate biomaterial or organic molecules.

In this study, a novel  $\beta$ -CD/siloxane hybrid polymer was synthesized from  $\beta$ -CD and (3-isocyanatopropyl) triethoxysilane. The resulting polysilsesquioxane, PSS- $\beta$ -CD, was characterized by <sup>13</sup>C and <sup>29</sup>Si nuclear magnetic resonance (NMR), infrared spectroscopy (IR) and X-ray diffraction (XRD). Thermal stability was examined by thermogravimetry (TGA). The capability of the hybrid polymer to form inclusion complexes was evaluated by complexation with phenolphthalein (PP), which was determined by the decrease of the PP solution absorbance, at  $\lambda = 550$  nm, in the presence of different PSS- $\beta$ -CD polymer amounts. As the color change of the indicator was not driven by pH changes, the semi empirical AM1 and DFT methods were employed to predict the geometry of the supramolecular complex, in order to correlate with

the experimental results, and the energetic profile of the process was calculated.

## Experimental

### Materials

$\beta$ -CD and (3-isocyanatopropyl)triethoxysilane, IPTS, were purchased from Aldrich Chemicals Co. Tin dibutylacetate (TBA) was obtained from Dow Corning (Midland, US). Phenolphthalein and sodium carbonate were obtained from Synth (São Paulo, Brasil). *N,N'*-dimethylformamide (DMF), acquired from Merck, was previously distilled at room pressure, and kept over 100 g L<sup>-1</sup> of a molecular sieve.  $\beta$ -CD was dried under vacuum (10<sup>-2</sup> mmHg) at 60 °C until a  $\beta$ -CD:water 1:1 molar ratio was obtained, as determined by TGA.

### Synthesis of PSS- $\beta$ -CD hybrid polymer

In a round bottom flask, 5 g of previously dried  $\beta$ -CD was dissolved in 30 mL of dried DMF at 50 °C under an inert atmosphere, to which 6.5 mL of IPTS was added (corresponding to a  $\beta$ -CD:IPTS molar ratio 1:6). The solution was kept under an inert atmosphere, with stirring for 72 h, giving rise to trialkoxysilane-modified  $\beta$ -CD with the molecular structure shown in Figure 1. To this solution, 0.50 mL of water and 1% (m/m) TBA were added and the flask was kept open under stirring until an increase in its viscosity was observed. Part of this viscous solution was poured into Teflon Petri dishes and kept in a wet chamber until the formation of a gel, followed by drying in the vacuum oven at 60 °C, giving rise to a resinous, fragile PSS- $\beta$ -CD film. Another part of the viscous solution was dried in a rotary evaporator at 50 °C for 72 h, followed by 72 h at 50 °C in a vacuum oven. This product was grounded and washed with a mixture of *n*-isopropyl alcohol/water (70%, v/v), at 30 °C for 48 h under magnetic stirring, to remove possible free  $\beta$ -CD.<sup>23</sup> Then the solid was allowed to settle and the solvent was discarded. This process was repeated three times. Finally, the resulting powdered hybrid polymer, PSS- $\beta$ -CD, (Figure 1), was dried under vacuum at 10<sup>-2</sup> torr at 60 °C for 72 h.

### Characterization

The structural characterization of PSS- $\beta$ -CD powdered hybrid polymer was performed by IR, solid state <sup>13</sup>C and <sup>29</sup>Si NMR and powder XRD. The infrared spectrum was recorded on a Bomem MB-Series Model B100, in the transmission mode between 4000 and 600 cm<sup>-1</sup> with resolution of

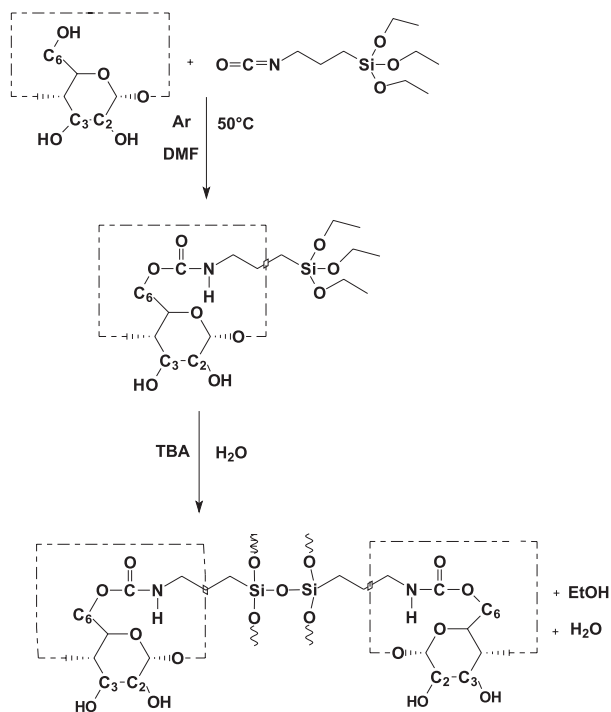


**Figure 1.** Schematic reaction of  $\beta$ -CD and IPTS and the hydrolysis and condensation reactions.

$4\text{ cm}^{-1}$ , using KBr pellets. Solid state  $^{13}\text{C}$  NMR spectrum was recorded on a Varian Inova 400 MHz spectrometer operating at 100 MHz, using the combination of cross-polarization, proton decoupling and magic angle spinning (CP/MAS). The  $^1\text{H}$  radio-frequency field strength was set to give a  $90^\circ$  pulse. Contact time and recycle delay were of 3 ms and 3 s, respectively. The chemical shift values were obtained in relation to adamantane, set at 38.9 ppm relative to tetramethylsilane (TMS).  $^{29}\text{Si}$  NMR spectrum was acquired in a Bruker Advance II operating in a 79.5 MHz, using a combination of high power decoupling method and magic angle spinning (HPDEC/MAS). The  $^1\text{H}$  radio-frequency field strength was set to give a  $90^\circ$  pulse and a time delay of 60 s. The chemical shifts were obtained in relation to caulinite, set at  $-91.2$  ppm relative to TMS. The powder XRD patterns were recorded on a Shimadzu X-ray diffractometer (XRD6000), using  $\text{Cu}(\text{K}\alpha)$  radiation ( $\lambda = 1.54060\text{ \AA}$ ), voltage of 40 kV and current of 30 mA. The thermal behavior of the PSS- $\beta$ -CD hybrid polymer was analyzed by TGA in a TA Instrument model 2950 with a heating rate of  $20\text{ }^\circ\text{C}/\text{min}$  over the temperature range of  $25\text{--}1000\text{ }^\circ\text{C}$ , under an argon flow.

The morphology of PSS- $\beta$ -CD film was observed by scanning electron microscopy (SEM) using a JEOL microscope, model JSM-6360LV, operating at 20 kV. Samples were fractured and covered with a thin film of a Pd/Au alloy in a high vacuum coater from Baltec, MED020.

### Availability of $\beta$ -CD in PSS- $\beta$ -CD polymer to form inclusion complexes

The ability of PSS- $\beta$ -CD polymer to form complexes was evaluated by the formation of an inclusion complex between  $\beta$ -CD and PP. This inclusion complex promotes a decrease of the absorption intensity of PP solutions.<sup>24</sup> Previously, a calibration curve was obtained in a water solution of PP,  $3 \times 10^{-5}\text{ mol L}^{-1}$ , in the presence of  $\beta$ -CD at 0.025, 0.10, 0.125, 0.15, 0.45, 0.75, 1.05 and  $1.35\text{ mol L}^{-1}$ . The pH of the PP solution was stabilized at 10.5 by the addition of  $4\text{ mmol L}^{-1}\text{ Na}_2\text{CO}_3$  in deionized water. The resulting solutions were measured in the wavelength range from 300 to 700 nm, with an Agilent HP 8453 UV-Vis instrument. The maximum absorbance was observed at a wavelength of 555 nm. All solutions were monitored at this wavelength at  $25\text{ }^\circ\text{C}$ . Powdered PSS- $\beta$ -CD polymer was added to 10 mL of a  $3 \times 10^{-5}\text{ mol L}^{-1}$  PP solution in different amounts from 0.80 to 13.0 mg. These mixtures were kept under magnetic stirring for 48 h and left at rest for settling of the polymer powder. The solution was removed, the pH was monitored and the spectrum of the powder was obtained.

### Swelling measurements of PSS- $\beta$ -CD film

Swelling measurements of the PSS- $\beta$ -CD film were performed in water following ASTM D471<sup>25</sup> to monitor water diffusion into the material. Film strips with dimensions of  $30\text{ mm} \times 10\text{ mm} \times 1\text{ mm}$  were previously weighed, in triplicate. Samples were immersed at regular intervals in deionized water and the surface of the swollen strip was gently dried with filter paper and immediately weighed. This procedure was repeated until a constant swollen weight was obtained. After, samples were dried in a vacuum oven at  $60\text{ }^\circ\text{C}$  for 72 h and immediately weighed again. The result is presented as an average of three measurements.

### Theoretical calculations

Equilibrium geometries for PP in different forms,  $\beta$ -CD and the inclusion complexes were optimized without any constraint using MM+<sup>26,27</sup> and then refined with the AM1 semi empirical model<sup>28</sup> as implemented in the HyperChem Evaluation Version.<sup>29</sup> In all cases the convergence criteria was  $10^{-3}\text{ kcal } \text{\AA}^{-1}\text{ mol}^{-1}$  in a conjugated algorithm. Thermal effects were estimated through the calculation of the hessian at the same semi empirical level assuming  $T = 298\text{ K}$  and  $P = 1.0 \times 10^5\text{ torr}$ . Results did not show any imaginary frequencies. Assuming these geometries, single point calculations at the BLYP<sup>30-32</sup> level were performed

with the mixed basis-set MBS2 suggested by Dos Santos and co-workers<sup>31</sup> constructed by the attribution of the 6-31++G(d,p)<sup>32-33</sup> basis set to O and O-H and the minimal basis set STO-3G<sup>34</sup> to C-H groups to solve the Kohn-Sham equations with a  $10^{-5}$  a.u. convergence criteria for the density change. For the BLYP/DFT calculations GAMESS-US<sup>35</sup> software was used.

## Results and Discussion

Figure 1 is a schematic representation of the synthetic route used for the preparation of PSS- $\beta$ -CD hybrid polymer. Based on the different nucleophilicities of hydroxyl groups in  $\beta$ -CD, with the C-OH from C-6 being more nucleophilic than others,<sup>1</sup> this C-OH must preferentially react with the 3-isocyanatopropyl group from IPTS. However, this synthesis was not conducted to be selective and other  $\beta$ -CD hydroxyls can compete in this reaction. A relevant fact to be considered, before the reaction, is control of the amount of residual water in the  $\beta$ -CD to avoid parallel reactions with the alkoxide and 3-isocyanatopropyl groups from IPTS. The hydrolysis and condensation of the intermediate  $\beta$ -CD-modified alkoxysilane gave rise to the PSS- $\beta$ -CD hybrid polymer. Figure 2 shows the IR spectra for the reagents and PSS- $\beta$ -CD hybrid polymer.

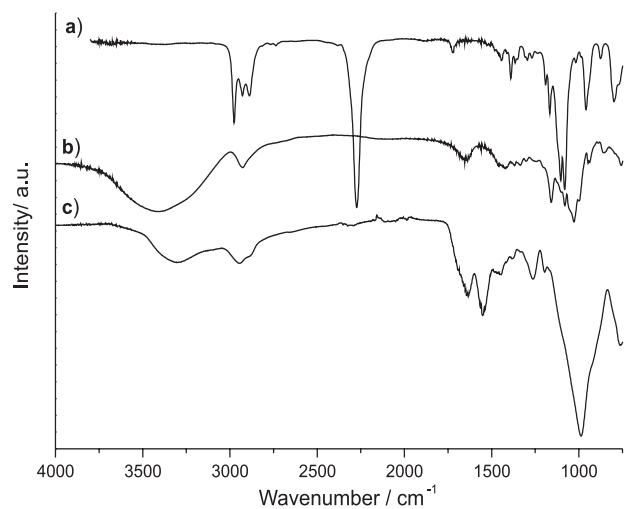


**Figure 2.** IR spectra for the reagents (a) IPTS and (b)  $\beta$ -CD, and product (c) PSS- $\beta$ -CD.

The infrared spectrum for IPTS shows an intense absorption of isocyanide groups at  $2270\text{ cm}^{-1}$  (Figure 2a), not observed in PSS- $\beta$ -CD hybrid polymer, which is an indication of the addition reaction between this group and  $\text{CH}_2\text{OH}$  during the initial reaction, or its hydrolysis at the final step of the reaction. In the PSS- $\beta$ -CD spectrum (Figure 2c) a very broad absorption centered at  $3284\text{ cm}^{-1}$  is

assigned to C-OH, N-H and Si-OH groups. The absorptions from  $2946$  to  $2860\text{ cm}^{-1}$  are associated to C-H from the propyl group and cyclodextrin units. The R-NH-CO-OR' secondary amide formed in the polymeric structure is characterized by Amide I (C=O bond) absorption at  $1692\text{ cm}^{-1}$ . Amide II is found at  $1548\text{ cm}^{-1}$ , as the main contribution of C-N and N-H motions, and Amide III at  $1263\text{ cm}^{-1}$ , associated to the mixed vibration involving OCN and N-H modes.<sup>36</sup> Finally, the strong and broad absorption centered at  $1000\text{ cm}^{-1}$  is assigned to C-O-C and Si-O-Si groups, this last from the polysilsesquioxane network, while the shoulder at  $920\text{ cm}^{-1}$  corresponds to Si-OH groups present at the end of the polymeric structure.<sup>39</sup>

Figure 3a shows the  $^{13}\text{C}$  NMR spectra for  $\beta$ -CD and PSS- $\beta$ -CD. The chemical shifts of the  $\beta$ -CD ring is also observed in the polymer. In the spectrum of the PSS- $\beta$ -CD hybrid polymer, the peak at 157 ppm is assigned to the C=O of the carbamate bond. Peaks at 12, 26 and 45 ppm are attributed to the C10, C9 and C8 carbons, respectively, from the propyl group introduced in the polymer from IPTS. These peaks are evidence of the formation of a covalent bond between siloxane and  $\beta$ -CD. An isocyanate peak at 122 ppm was not observed.

Figure 3B shows the  $^{29}\text{Si}$  NMR spectrum of PSS- $\beta$ -CD hybrid polymer. This polymer presents different Si (T) sites, which is evidence of incomplete condensation of the siloxane network, such as: T<sup>3</sup>, associated to the peak at  $-67\text{ ppm}$ ; T<sup>2</sup> at  $-58\text{ ppm}$ , T<sup>1</sup> at  $-50\text{ ppm}$  and T<sup>0</sup> at  $-44\text{ ppm}$ . The T<sup>0</sup> site corresponds to the hydrolyzed intermediate, with no condensed Si-OH groups. This site can be observed only in the presence of a large voluminous substituent at Si, such as  $\beta$ -CD. The presence of T<sup>0</sup> in the product suggests that the  $\beta$ -CD promotes steric hindrance, or that there are associations by hydrogen bonds between Si-OH (from the siloxane network) and C-OH (from  $\beta$ -CD), which make the condensation reaction difficult.

The diffractograms of  $\beta$ -CD and PSS- $\beta$ -CD can be seen in Figure 4.  $\beta$ -CD is a highly crystalline material with main diffractions at  $9.1$ ,  $12.5$  and  $22.7^\circ$  ( $2\theta$ ). PSS- $\beta$ -CD showed an amorphous pattern with two halos centered at  $11^\circ$  and  $21^\circ$  ( $2\theta$ ). No diffractions from crystalline  $\beta$ -CD were found in the polymer, suggesting that the distribution of  $\beta$ -CD in the polymeric chains avoids the formation of aggregates.

PSS- $\beta$ -CD film is transparent, vitreous, brittle and homogeneous. A SEM micrograph of the film surface can be seen in Figure 5. This film presents a globular morphology with low roughness, with no pores or phase separation.

PSS- $\beta$ -CD thermal behavior was evaluated by TGA and the result is compared with that for  $\beta$ -CD, as can be seen in Figure 6. The weight loss observed in  $\beta$ -CD and PSS- $\beta$ -CD

up to 100 °C mainly corresponds to residual water loss.  $\beta$ -CD has a fast thermal degradation centered at 340 °C. Above 400 °C the residue degrades up to 900 °C. A different

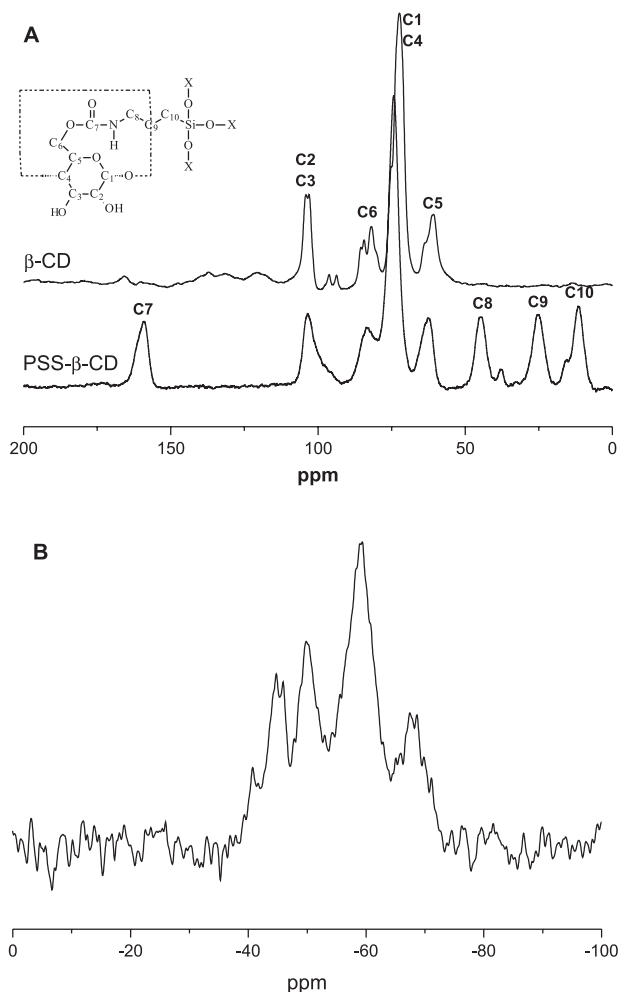


**Figure 3.** (A)  $^{13}\text{C}$  NMR spectra for  $\beta$ -CD and PSS- $\beta$ -CD and (B)  $^{29}\text{Si}$  NMR spectrum for PSS- $\beta$ -CD.

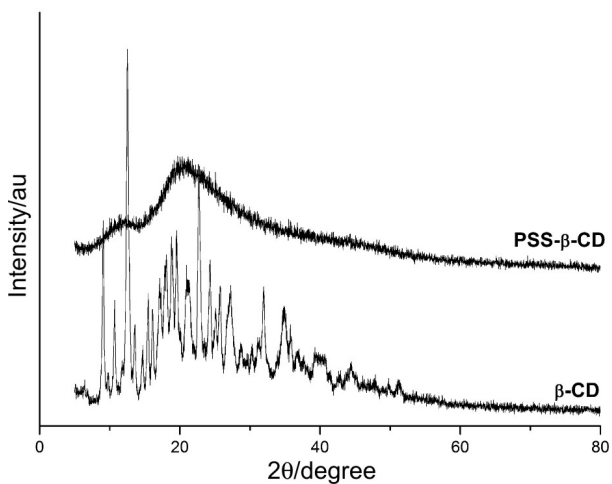


**Figure 4.** X ray diffractograms.

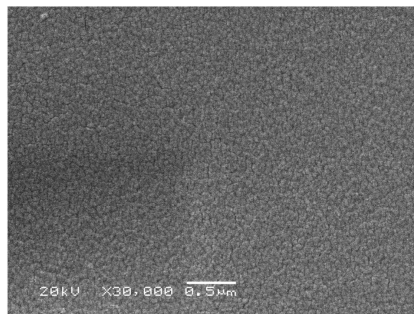


**Figure 5.** SEM micrograph of PSS- $\beta$ -CD.

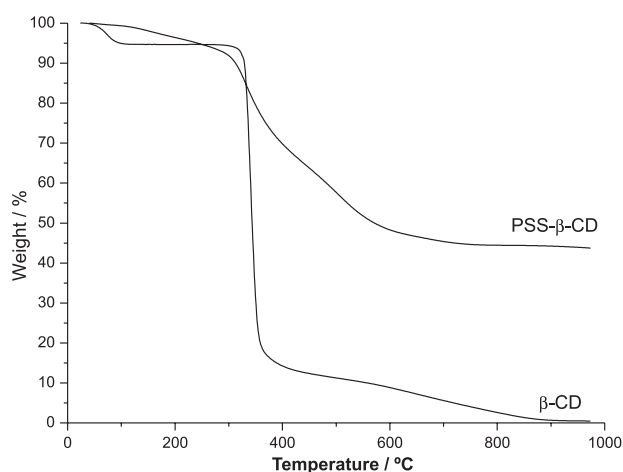


**Figure 6.** Weight (%) versus temperature from TGA of  $\beta$ -CD and PSS- $\beta$ -CD.

thermal behavior is observed for PSS- $\beta$ -CD. Volatiles are lost up to 100 °C associated to the water residues trapped in the polymer (2% m/m). The polymer then starts degrading at 180 °C with desamination and decarbamation of the sample, followed by degradation of  $\beta$ -CD and the propyl groups, up to 400 °C. At this temperature mineralization starts producing a residue of 35% of  $\text{SiC}_x\text{O}_y$  at 950 °C.<sup>40</sup>

Swelling capability is an important property to be studied to check how permeable is the matrix to water in order to transport guest solutes to the  $\beta$ -CD cavity. The swelling ratio  $S_R$ , was determined by equation 1, where  $m_s$  is the mass of the swollen sample at equilibrium and  $m_d$  is the mass of the dried sample after swelling.

$$S_R = (m_s - m_d) / m_d \quad (1)$$

The results (not shown) show that the PSS- $\beta$ -CD film presents a fast swelling in water, reaching its maximum capability at approximately 30 min, with a mass increase of 32.6%. This behavior can be explained not only by the presence of  $\beta$ -CD, which contains a high content of OH groups, but also by the presence the Si-OH groups in the material, as shown by  $^{29}\text{Si}$  NMR ( $T^2$ ,  $T^1$  and  $T^0$  peaks). These

sites, opposing the T<sup>3</sup> siloxane site, can interact with water by hydrogen bonds. Additionally, as shown in the XRD, the polymer is amorphous, favoring swelling.

Phenolphthalein, a typical acid-alkaline indicator dye, exhibits the equilibrium shown in Figure 7. It is commonly used as a pH indicator that changes color from colorless to red when a neutral solution becomes alkaline.

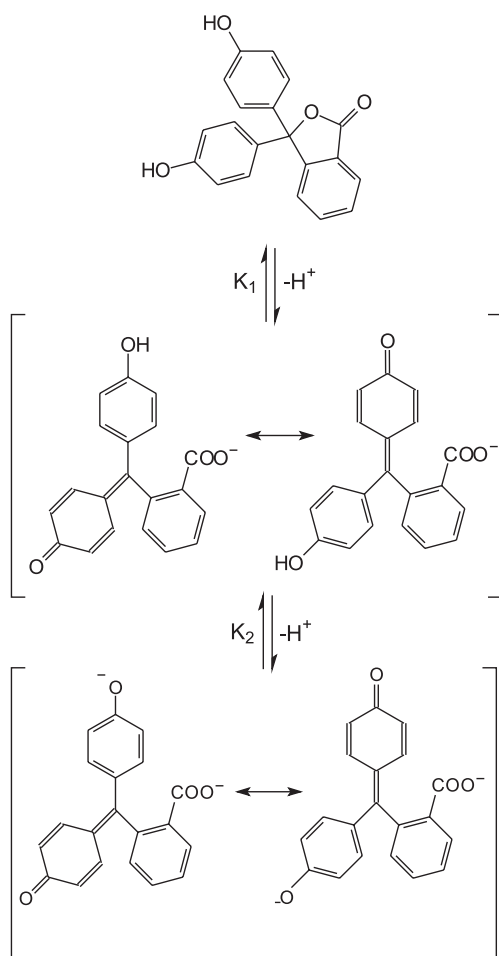


**Figure 7.** Schematic representation of acid dissociation equilibrium of PP.

A supramolecular complex between PP and  $\beta$ -CD is highly stable and its formation changes the color of PP alkaline solutions. An alkaline solution of PP discolors rapidly when  $\beta$ -CD is added and the extent of color fading is proportional to the concentration of  $\beta$ -CD added. Taguchi<sup>42</sup> studied the complex formation between  $\beta$ -CD and PP by UV-Vis absorption spectra and <sup>13</sup>C NMR spectra and proposed that when the red ionized form of PP is enclosed in  $\beta$ -CD, it is forced into its lactone structure, without protonating the phenolic groups. He suggested two possibilities to explain the structure of PP in the cavity of  $\beta$ -CD: the first is when one of the phenolate groups is into the cavity and the other, together with the aryl residue

that bears the lactone ring are out of the cavity. The other possibility is when the aryl residue with the lactone ring is inside the cavity and the two phenolate rings rest out of the cavity. In order to determine the ability of  $\beta$ -CD to form complexes when grafted in the PSS- $\beta$ -CD hybrid polymer, a PP solution was used as a probe and was revealed to be very suitable for such an investigation. Figure 8A shows the UV-Vis spectra of PP solutions in equilibrium with different PSS- $\beta$ -CD amounts. It is noticeable that the maximum PP absorbance at 555 nm decreases with the increase of PSS- $\beta$ -CD amount, which is evidence of the presence of available  $\beta$ -CD to form complexes within the polymer. In order to quantify the available amount of  $\beta$ -CD present in the PSS- $\beta$ -CD polymer to form the inclusion complex, a calibration curve was constructed with the addition of different amounts of pure  $\beta$ -CD to PP solution. The stoichiometric ratio of this complex and the binding constant, *K*, were determined from spectrophotometric data, using Scott's equation.<sup>41,40</sup>

$$C_{\beta\text{-CD}}/\Delta A = C_{\beta\text{-CD}}/(C_{\text{PP}} \times \Delta\varepsilon) + 1/(C_{\text{PP}} \times \Delta\varepsilon \times K) \quad (2)$$

Where  $C_{\beta\text{-CD}}$  and  $C_{\text{PP}}$  are the total molar concentrations of  $\beta$ -CD and PP, respectively,  $\Delta A$  is the change in the absorbance after addition of  $\beta$ -CD ( $\Delta A = A_{\text{PP}} - A_{\beta\text{-CD,PP}}$ ), *K* is the binding constant and  $\Delta\varepsilon$  is the difference of the molar absorptivities for free and complexed phenolphthalein. If the resulting plot of  $C_{\beta\text{-CD}}/\Delta A$  against  $C_{\beta\text{-CD}}$  yields a straight line, a 1:1  $\beta$ -CD: PP complex is expected and the binding constant *K* (mol L<sup>-1</sup>) can be calculated. Figure 8B shows the plot  $C_{\beta\text{-CD}}/\Delta A$  against  $C_{\beta\text{-CD}}$  that yielded a straight line with a good correlation factor (*R* = 0.998) suggesting a  $\beta\text{-CD} + \text{PP} \rightleftharpoons \beta\text{-CD}\cdot\text{PP}$  equilibrium model. Similarly, an excellent linear plot confirms the 1:1 stoichiometric ratio of the investigated complex.<sup>43</sup>

Table 1 shows the binding constant (*K*), obtained by equation 2, and the variation of the molar absorptivities ( $\Delta\varepsilon$ ) between pure PP solution and  $\beta$ -CD-PP complex

**Table 1.** Variation of molar absorptivities ( $\Delta\varepsilon$ ) between pure PP solution and  $\beta$ -CD-PP complex solution. Binding constant (*K*) calculated from Scott's equation (equation 2)

$C_{\beta\text{-CD}}$	$\Delta\varepsilon$	<i>K</i> (mol L <sup>-1</sup> )
0.000		
0.025	0.0111	1.21 × 10 <sup>4</sup>
0.050	0.0174	
0.100	0.0265	
0.125	0.0272	
0.150	0.0320	
0.450	0.0861	
0.750	0.1175	
1.050	0.1556	
1.350	0.2007	

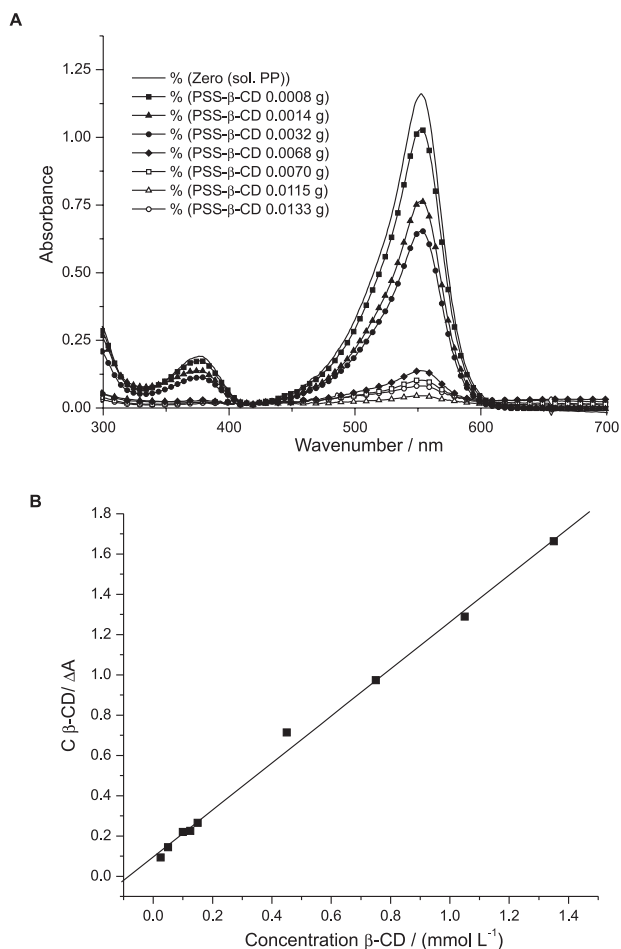


**Figure 8.** (A) Absorption spectra of PP solutions in equilibrium with different PSS- $\beta$ -CD amounts and (B) Plot of the equation  $C_{\beta\text{-CD}}/\Delta A$  versus  $C_{\beta\text{-CD}}$ .

solution. The binding constant found for this system at the temperature of 25 °C is in agreement with literature values: 1 to  $3 \times 10^4$  mol L<sup>-1</sup>.<sup>41, 42</sup>

Absorbance was also measured in PP solutions in equilibrium with different PSS- $\beta$ -CD amounts. The equivalent amount of available  $\beta$ -CD in the PSS- $\beta$ -CD polymer for the formation of the inclusion complex can be seen in Table 2.

**Table 2.** PSS- $\beta$ -CD amount in the PP solution, absorbance of this solution measured at  $\lambda = 555$  nm and the equivalent amount of available of  $\beta$ -CD in the PSS- $\beta$ -CD polymer to form the inclusion complex

PSS- $\beta$ -CD amount (mg)	A ( $\lambda = 555$ nm)	Equivalent amount of $\beta$ -CD in PSS- $\beta$ -CD (mmol L <sup>-1</sup> )
0.00	1.161	
0.08	1.031	0.011
0.14	0.768	0.026
0.32	0.653	0.031
0.68	0.138	0.045
1.15	0.081	0.046
1.33	0.045	0.046

The amount of available  $\beta$ -CD to form an inclusion complex in the PSS- $\beta$ -CD hybrid polymer increases with the amount of the polymer added to PP solution in a non linear behavior. However, the quantification of  $\beta$ -CD in the polymer is complex because it is not possible to estimate the molar mass of the hybrid polymer. Considering these results and the swelling capability of the PSS- $\beta$ -CD hybrid films, it can be inferred that steric hindrance is the main factor for the non linear behavior of the color fading in PP solutions in the presence of PSS- $\beta$ -CD hybrid polymer. Obviously,  $\beta$ -CD grafted in the polymer promotes a random steric hindrance and no distribution profile can be found with the evaluations performed.

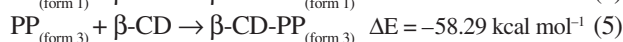
In order to evaluate the conformation of the PP included in the  $\beta$ -CD and to understand the inclusion reaction thermodynamics, we have developed semi empirical and *ab initio* calculations for the precursors and the inclusion complexes.

The geometry of the colorless PP form obtained using AM1 is in very good agreement with reported bond distances and angles,<sup>41</sup> as can be seen in Figure 9A (black is the geometry obtained from crystallographic data). The differences can be attributed to the freedom of the aryl rings in the vacuum calculations. Even though there is no crystallographic data for the opened ring form (the gray one) we assumed the calculated structure as the most stable one.

As far as we know, the literature has not a good structural explanation for such color change driven by complexation. The previous work of Taguchi<sup>42</sup> shows that the alkaline red form of PP is converted into the colorless lactone form by interaction with  $\beta$ -CD without change in the pH. As described before, in spite of the form of PP considered, there are only two possibilities for the inclusion complex to be formed: through the phenolate and through the carboxylic (or lactone) phenyl rings. We performed AM1 geometry optimizations starting with these four different possibilities that are described in Figure 9B. Complexes **1** and **2** are the PP colored forms and the others (**3** and **4**) are the colorless ones.

Structures **2** and **4** did not converge to inclusion complexes but to clearly hydrogen bonded structures formed between the carboxylic/lactone and  $\beta$ -CD-OH external groups. Structures **1** and **3** converged to inclusion complexes and so we performed BLYP/DFT single point calculations to estimate the energy profile of the reaction. The total energies can be seen in Table 3.

These DFT data can be used to calculate the energy variation for the following reactions:



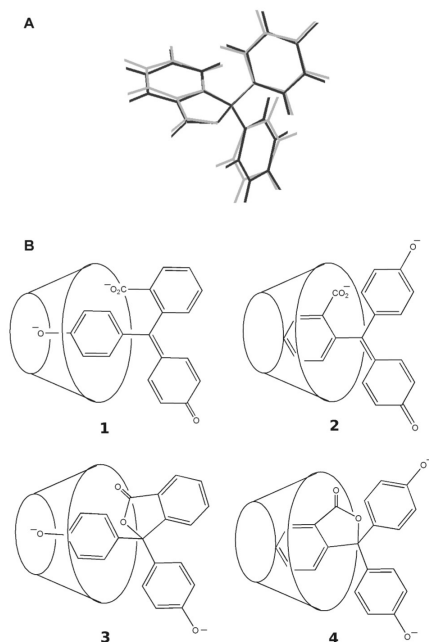


**Figure 9.** (A) Comparison between the experimental (black) geometry of the PP lactanoid form and the AM1 optimized structure (gray) and (B) schematic representations of the inclusion complexes studied theoretically in this work.

**Table 3.** Total energies calculated for the free PP forms and  $\beta$ -CD and the supramolecular complexes

Structure	Total Energies / a.u.*	
	AM1	DFT
$\beta$ -CD	-645.5736	-4240.2122
PP (form A)	-147.2369	-1060.4556
PP (form C)	-147.2302	-1060.4276
Complex A	-792.8596	-5300.7360
Complex C	-792.8659	-300.7327

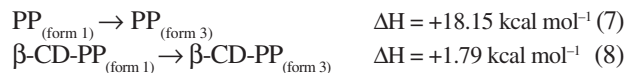
\* conversion to kcal mol<sup>-1</sup> by a 627.51 factor.

As one can clearly see, the inclusion reactions are exothermic and the inclusion of the lactanoid form is favored by more than 15 kcal mol<sup>-1</sup>. In spite of that, we have to take into account the endothermic conversion of the form **1** into **3** (closure of the lactanoid ring) and when this is done, a thermodynamic cycle can be closed with the reaction:



Comparison of equations 3 and 6 shows that the inclusion favors the formation of the colorless PP form, as compared to the free PP conversion. The difference is exactly the extra stabilization of the included form **3**. The same conclusions can be obtained if the semi empirical AM1 data are used. As expected by experiment, the conversion

of the free form is unfavorable but the conversion of the included form has also a positive  $\Delta E$  value (equation 6). To solve this problem we have estimated thermal effects by the calculation of enthalpy differences for equations 3 and 6, using vibrational analyses of all species at AM1 level. These enthalpies were added to DFT energies and the results are shown in equations 7 and 8.



As can be clearly seen, thermal effects estimated by this semi empirical method decrease the energy for the conversion of included PP by 0.3 kcal mol<sup>-1</sup> and increase the value for the free species by 0.6 kcal mol<sup>-1</sup>. Although these last results did not show a negative value for the conversion of included PP, they confirm that the conversion is facilitated by the inclusion process in spite of the low quality of semi empirical calculations for the estimation of vibrational data (and thermal ones as a consequence). Taking into account that the product  $kT$  (4 kcal mol<sup>-1</sup> at 298 K) is a good estimation of thermal energy for the system, we can understand the spontaneity of the conversion of included species as well as thermal energy overcome the energy for the conversion by *ca.* 2 kcal mol<sup>-1</sup>.

Figure 10 shows the optimized supramolecular structure and it is easily seen that the hydrogen bonds play a remarkable role in its stabilization. Inclusion through the phenolate rings maximizes the number of hydrogen bonds and the average distance between the phenolate oxygen and  $\beta$ -CD hydrogens is 2.2 Å. This may be the reason why inclusion through forms **2** and **4** is not favored.

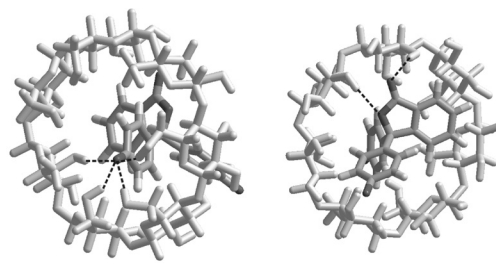


**Figure 10.** Two views of the optimized structure obtained for the inclusion complex between  $\beta$ -CD and the PP lactanoid form. Left: along the smaller side of  $\beta$ -CD showing O-H proximity; Right: along the greater side of  $\beta$ -CD showing the interaction between the lactanoid ring and the  $\beta$ -CD molecule.

The theoretical results give us insight into the favorable closure of PP in the presence of  $\beta$ -CD. As one can see in equation 4, the inclusion of the red form of PP is exothermic and the geometry obtained by calculation is very similar to the one shown in Figure 10, the only difference being the



carboxylate group. One hypothesis is that the supramolecular complex formed by the red form (form **1**) and  $\beta$ -CD seems to constrain the PP geometry and to act as a template site in order to put the carboxylic group in the right position (through hydrogen bonds) to close the lactanoid ring. Once the complex is formed, the closure of the ring is favorable and the formation of the colorless PP form is experimentally observed.

## Conclusions

PSS- $\beta$ -CD hybrid polymer, obtained as a rigid and non crystalline material, typical of polysilsesquioxane resins, showed relatively good water permeability, characterized by the swelling degree. Therefore, water molecules can transport guest molecules to complex with the cavity of  $\beta$ -CD bonded to the polymeric chain. This was verified by the complexation of phenolphthalein into the cavity of  $\beta$ -CD, which was shown by the change in the color of the solution from red to colorless, without changes in the pH. A 1:1 inclusion complex was verified for PP: $\beta$ -CD. Theoretical results indicated that the colorless form is favored, due to the inclusion of the phenolate ring into the  $\beta$ -CD cavity and the formation of hydrogen bonds seems to be the enthalpic driving force of the reaction.

## Acknowledgments

We gratefully acknowledge financial support from FAPESP (Proc. No. 03/09926-1) and CNPq (Proc. 305916/2006-8). The authors also thank Prof. Dr. Carol H. Collins for English revision. Camilla Abbehausen thanks Dow Corning do Brazil for support.

## References

1. Szejtli, J.; *Chem. Rev.* **1998**, *98*, 1743.
2. Tatsuya, S.; *Jpn. Pat.* 11209787, 1999.
3. Mongkolkul, P.; Rodart, P.; Pipatthitikorn, T.; Meksut, L.; Sanguandeeikul, R.; *J. Inclusion Phenom. Macrocyclic Chem.* **2006**, *56*, 167.
4. Mura, P.; Faucci, M. T.; Parrini, P. L.; Furlaneto, S.; Puinzausti, S.; *Int. J. Pharm.* **1999**, *179*, 117.
5. Ramírez, H. L.; Valdivia, A.; Cao, R.; Torres-Labandeira, J. J.; Fragoso, A.; Villalonga, R.; *Bioorg. Med. Chem. Lett.* **2006**, *16*, 1499.
6. Zhou, S.; Wang, L.; Zhang, A.; Lin, K.; Liu, W.; *J. Agric. Food Chem.* **2008**, *56*, 2708.
7. Fontanova, E.; Di profio, G.; Crucio, E.; Giorno, L.; Driolli, E.; *J. Inclusion Phenom. Macrocyclic Chem.* **2007**, *57*, 537.
8. Allabashi, R.; Arkas, M.; Hormann, G.; Tsiourvas, D.; *Water Res.* **2007**, *41*, 476.
9. Khan, A. R.; Forgo, P.; Stine, K. J.; D'Souza, V. T.; *Chem. Rev.* **1998**, *98*, 1977.
10. Berto, S.; Bruzzonitti, M. C.; Cavalli, R.; Perrachon, D.; Prenesti, E.; Sarzanini, C.; Trtta, F.; Tumiatti, W.; *J. Inclusion Phenom. Macrocyclic Chem.* **2007**, *57*, 631.
11. Kim, I. W.; Choi, H. M.; Yoon, H. J.; Park, J. H.; *Anal. Chim. Acta* **2006**, *569*, 151.
12. Yi, J. M.; Tang, K.W.; *J. Chromatogr. A* **2000**, *883*, 137.
13. Wang, X.; Zeng, H.; Wei, Y.; Lin, J. M.; *Sens. Actuators, B* **2006**, *114*, 565.
14. Choi, H. S.; Ooya, T.; Sasaki, S.; Yui, N.; *Macromolecules* **2003**, *36*, 5342.
15. Arima, H.; Kihara, F.; Hirayama, F.; Uekama, K.; *Bioconjugate Chem.* **2002**, *13*, 1211.
16. Mark, J. E.; Allcock, H. R.; West, R.; *Inorganic Polymers*, Prentice Hall: Englewood Cliffs, NJ, 1992.
17. Tanaka, K.; Inafuku, K.; Chujo, Y.; *Bioorg. Med. Chem.* **2008**, *16*, 10029.
18. Masuda, T.; Yamamoto, S.; Moriya, O.; Kashio, M.; Sugizaki, T.; *Polym. J.* **2008**, *40*, 1042.
19. Dave, B. C.; Dunn, B.; Valentine, J. S.; Zink, J. I.; *Anal. Chem.* **1994**, *66*, 1120.
20. Mena, B.; Herrero, M.; Rives, V.; Lavrenko, M.; Eggers, D. K.; *Biomaterials* **2008**, *29*, 2710.
21. Avnir, D.; Coradin, T.; Lev, O.; Livage J.; *J. Mater. Chem.* **2006**, *16*, 1013.
22. Gill, I.; Ballesteros, A.; *J. Am. Chem. Soc.* **1998**, *120*, 8587.
23. Chatjigakis, A. K.; Donze, C.; Coleman, A. W.; Cardot, P.; *Anal. Chem.* **1992**, *64*, 1632.
24. Vélaz, I.; Isasi, J. R.; Sánchez, M.; Uzqueda, M.; Ponchel, G.; *J. Inclusion Phenom. Macrocyclic Chem.* **2007**, *57*, 65.
25. Standard Test Methods for Vulcanized Rubber and Thermoplastic elastomers-effects of liquids, *Annual Book of Standards*, **1998**, ASTM D 412-98.
26. MM+ force field is an extension of MM2 implemented in HyperChem software.
27. Allinger, N. L.; *J. Am. Chem. Soc.* **1977**, *99*, 8127.
28. Dewar, M. J. S.; Zoebisch, E. G.; Healy, E. F.; Stewart, J. J. P.; *J. Am. Chem. Soc.* **1985**, *107*, 3902.
29. HyperChem Professional 8.0, Hypercube, Inc. 1115 NW 4th St. Gainesville, FL 32601, USA.
30. Miehllich, B.; Savin, A.; Stoll, H.; Preuss, H.; *Chem. Phys. Lett.* **1989**, *157*, 200.
31. Anconi, C. P. A.; Nascimento, C. S.; De Almeida, W. B.; Dos Santos, H. F.; *J. Braz. Chem. Soc.* **2008**, *19*, 1033.
32. Hehre, W. J.; Ditchfield, R.; Pople, J. A.; *J. Chem. Phys.* **1972**, *56*, 2257.
33. Clark, T.; Chandrasekhar, J.; Spitznagel, G.W.; Schleyer, P. von R.; *J. Comput. Chem.* **1983**, *4*, 294.
34. Hehre, W. J.; Stewart, R. F.; Pople, J.A.; *J. Chem. Phys.* **1969**, *51*, 2657.

35. Schmidt, M. W.; Baldrige, K. K.; Boatz, J. A.; Elbert, S. T.; Gordon, M. S.; Jensen, J. H.; Matsunaga, S. K. N.; Nguyen, K. A.; Su, S.; Windus, T. L.; Dupuis, M.; Montgomery, J. A. Jr.; *J. Comput. Chem.* **1993**, *14*, 1343.
36. Bellamy, L. J.; *The Infrared Spectra of Complex Molecules*, Wiley: New York, 1966.
37. Smith, A. L.; *Analysis of Silicones*, Wiley: New York, 1991.
38. Zarzycki, P. K.; Lamparczyk, H.; *J. Pharm. Biomed. Anal.* **1998**, *18*, 165.
39. Taguchi, K.; *J. Am. Chem. Soc.* **1986**, *108*, 2705.
40. Scott, R. L.; *Rec. Trav. Chim.* **1956**, *75*, 187.
41. Fitzgerald, L. J.; Gerkin, R. E.; *Acta Crystallogr., Sect C: Cryst. Struct. Commun.* **1998**, *54*, 535.

*Submitted: November 25, 2009*

*Published online: June 23, 2010*

**FAPESP helped in meeting the publication costs of this article.**